CHEMISTRY OF MATERIALS
Article

Chem. Mater. **2010,** *22,* 5319–5327 5319
DOI:10.1021/cm1016245

Covalent Grafting of *m*-Phenylene-Ethynylene Oligomers to Oxide Surfaces

Justin M. Notestein,*,† Christian Canlas,† John Siegfried,† and Jeffrey S. Moore‡

†*Department of Chemical and Biological Engineering, Northwestern University, Evanston, Illinois 60208, and* ‡*Department of Chemistry, University of Illinois Urbana−Champaign, Urbana, Illinois 61801*

Received June 10, 2010. Revised Manuscript Received August 6, 2010

Oligomeric phenylene ethynylene is potentially a useful molecule for organic photovoltaics, light emitting diodes, sensor materials, or as intrinsically porous polymers for gas storage and separation. In the former two applications, the organic molecules are supported on an inorganic material for structural support or for charge collection at an electrode. Here, a 12 repeat unit oligomer of m-phenylene ethylene is covalently attached to high surface area and planar oxide supports as an alternate route to materials development, which displays novel properties and applications due to the covalent connection to the surface. Oligomers and model dimers are attached to alkyl-azide decorated surfaces via Cu-catalyzed 1,3-dipolar Huisgen cycloaddition or covalently linked with silane-bearing surfaces via Rh-catalyzed hydrosilylation. Surface structures and densities are verified by FTIR, TGA, transmission UV−visible spectroscopy, N_2 physisorption, and transmission electron microscopy. On high-surface-area materials, hydrosilylation routes yield loadings up to 0.09 molecules nm^{-2}, whereas on planar surfaces, densities reach 0.22 molecules nm^{-2}, comparable to the footprint of the extended Tg side groups. Grafted molecules retain the solvation-dependent "folding" behavior of soluble oligomers as determined by solvent- and temperature-dependent photoluminescence spectra of grafted oligomers suspensions. Grafted oligomers can be suspended in liquids in which the oligomers are not intrinsically soluble, demonstrating, for example, that dodecane and decalin have opposite association behavior, in spite of both their very low polarity parameters. Photoluminescence spectra are consistent with coexisting folded and unfolded oligomers when grafted, in contrast with highly cooperative changes in solution. Highly loaded surfaces show significant hysteresis upon heating, suggesting a kinetic as well as thermodynamic solvent effect. Pinene guest molecules enhance folding of the grafted oligomers, demonstrating a responsive adsorbent surface. Having demonstrated proof of concept, covalently grafted oligo(PE) materials are applicable as a new class of tunable adsorbent materials and optoelectronic materials.

Introduction

Oligomeric phenylene ethynylene species deposited onto surfaces have applications as OLEDs, organic PV materials, and sensors.[1,2] Similar oligomeric structures have also been grown inside mesoporous materials,[3] or had the oxide grown around it.[4] These materials are typically constructed from oligo(*p*-phenylene ethynylene). In contrast to the straight-chain para-linked isomer, oligo(*m*-phenylene-ethynylene)s, oligo(mPE), exist as dendritic and linear architectures with potential applications as intrinsically porous polymers for gas storage and separation,[5] light-harvesting molecules, or for signal amplification.[2,6] As linear oligomers, these molecules display reversible folding to form cavity-containing helices with host−guest properties.[7−9] This latter behavior is driven by solvophobic $\pi-\pi$ stacking,[10−12] which also contributes to the molecule's electronic properties.[13]

*Corresponding author. E-mail: j-notestein@northwestern.edu.

(1) Pinto, M. R.; Schanze, K. S. *Synthesis* **2002**, 1293–1309. Hatchett, D. W.; Josowicz, M. *Chem. Rev.* **2008**, *108*, 746–769. Mwaura, J. K.; Zhao, X. Y.; Jiang, H.; Schanze, K. S.; Reynolds, J. R. *Chem. Mater.* **2006**, *18*, 6109–6111. Kim, K.; Webster, S.; Levi, N.; Carroll, D. L.; Pinto, M. R.; Schanze, K. S. *Langmuir* **2005**, *21*, 5207–5211. Wosnick, J. H.; Liao, J. H.; Swager, T. M. *Macromolecules* **2005**, *38*, 9287–9290. Benanti, T. L.; Venkataraman, D. *Photosynthesis Res.* **2006**, *87*, 73–81. Hoppe, H.; Sariciftci, N. S. *J. Mater. Res.* **2004**, *19*, 1924–1945. Zhu, D. F.; He, Q. G.; Cao, H. M.; Cheng, J. G.; Feng, S. L.; Xu, Y. S.; Lin, T. *Appl. Phys. Lett.* **2008**, 93. Moon, J. H.; McDaniel, W.; Hancock, L. F. *J. Colloid Interface Sci.* **2006**, *300*, 117–122. Ho, S. W.; Kwei, T. K.; Vyprachticky, D.; Okamoto, Y. *Macromolecules* **2003**, *36*, 6894–6897. Arnt, L.; Tew, G. N. *Langmuir* **2003**, *19*, 2404–2408.
(2) Thomas, S. W.; Joly, G. D.; Swager, T. M. *Chem. Rev.* **2007**, *107*, 1339–1386.
(3) Ogawa, K.; Chemburu, S.; Lopez, G. P.; Whitten, D. G.; Schanze, K. S. *Langmuir* **2007**, *23*, 4541–4548.
(4) Clark, A. P. Z.; Shen, K. F.; Rubin, Y. F.; Tolbert, S. H. *Nano Lett.* **2005**, *5*, 1647–1652.
(5) Cooper, A. I. *Adv. Mater.* **2009**, *21*, 1291–1295. Tolusa, J.; Kub, C.; Bunz, U. H. F. *Angew. Chem., Int. Ed.* **2009**, *48*, 4610–4612. Bharathi, P.; Moore, J. S. *Macromolecules* **2000**, *33*, 3212–3218.
(6) Bunz, U. H. F. *Chem. Rev.* **2000**, *100*, 1605–1644. Kim, J.; Swager, T. M. *Nature* **2001**, *411*, 1030–1034.
(7) Prince, R. B.; Barnes, S. A.; Moore, J. S. *J. Am. Chem. Soc.* **2000**, *122*, 2758–2762.
(8) Tanatani, A.; Hughes, T. S.; Moore, J. S. *Angew. Chem., Int. Ed.* **2001**, *41*, 325. Tanatani, A.; Mio, M. J.; Moore, J. S. *J. Am. Chem. Soc.* **2001**, *123*, 1792–1793.
(9) Hill, D. J.; Mio, M. J.; Prince, R. B.; Hughes, T. S.; Moore, J. S. *Chem. Rev.* **2001**, *101*, 3893–4011. Arnt, L.; Tew, G. N. *Macromolecules* **2004**, *37*, 1283–1288. Smaldone, R. A.; Moore, J. S. *Chem.—Eur. J.* **2008**, *14*, 2650–2657.
(10) Nelson, J. C.; Saven, J. G.; Moore, J. S.; Wolynes, P. G. *Science* **1997**, *277*, 1793–1796.

Published on Web 08/26/2010

Using two approaches, oligo(mPE) has been covalently grafted to alkyl-azide decorated silica surfaces via Cu-catalyzed 1,3 dipolar Huisgen cycloaddition or covalently grafted to SiH-bearing surfaces via Rh-catalyzed hydrosylation (Scheme 1). Although both techniques have been used to create covalently functionalized surfaces in the past,[14,15] current work is novel for its use of the large, and dynamic, conjugated oligo(mPE) molecules, and covalent immobilization onto high surface area and mesoporous oxide materials. Such materials are preferred over planar substrates for applications such as sensing, adsorption, and sensitized solar cells.

These relatively large oligomers are grafted at moderate surface densities and they retain their solvophobic association properties when grafted to oxide surfaces. Advantageously, the covalent connection of these conjugated host molecules to bulk particles allows these molecules to be exposed to liquid environments in which they would not normally be soluble, such as water or alkanes, which allows scientific insights into the nature of aggregation and guest binding on surfaces and may enable future separations, electronics, or sensing applications.

Scheme 1. Structure of the 12-Repeat Unit Oligomer (12mer) and the Model (dimer) and the Retrosynthesis for Surface Attachment (mPE-CCH indicates an ethylene-terminated oligo(mPE))

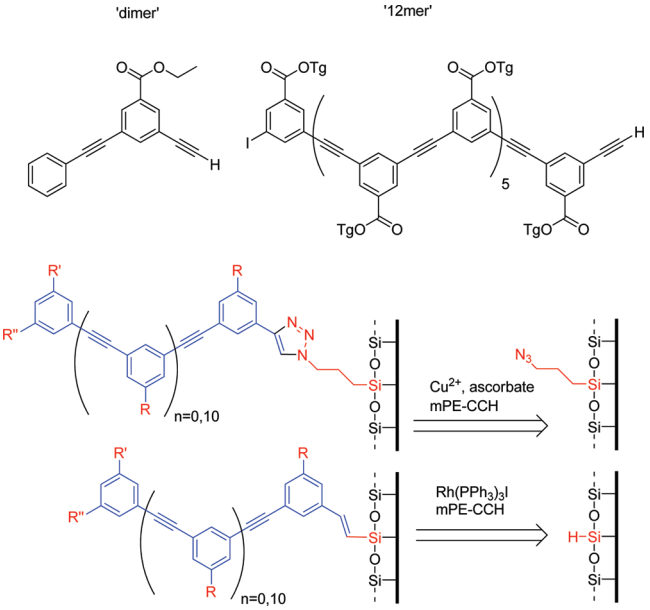

Experimental Methods

Molecular Precursors and Supports. As shown in Scheme 1, oligomers of *m*-phenylene-ethynylene consisted of a 12mer of Tg-3,5-diethynylbenzoate prepared using published solid-phase Pd-catalyzed Sonogashira coupling,[16] or a dimer prepared in four steps from 3-bromo-5-iodo-benzoic acid, ethanol, trimethylsilyl acetylene, and phenyl acetylene using established Pd-catalyzed Sonogashira coupling. The 12mer and dimer both possess one terminal acetylene deprotected in a final synthesis step. Powders (silica gel with 500 $m^2\ g^{-1}$, ~16 nm diameter Si_3N_4 nanoparticles with 110 $m^2\ g^{-1}$, and 7 nm pore diameter MSU mesostructured silica with 750 $m^2\ g^{-1}$) were washed in 10−20 volume equivalents each of 1:1 HCl/MeOH, H_2O, concentrated H_2SO_4, and H_2O again until washes run neutral to remove surface contamination and metals. The Si_3N_4 nanoparticles possess a native oxide surface that was used for functionalization in subsequent steps. Powders were dried at 120 °C under dynamic vacuum for >12 h to remove physisorbed water. Quartz plates (Chemglass) were sonicated in their corresponding solutions and dried under a stream of dry N_2. Unless otherwise mentioned, precursor chemicals and solids were obtained from Sigma-Aldrich at the highest available purity. For materials synthesis, solvents were dried using recommended practices.[17]

Grafting by Coupling. Functional silanes 3-(azidopropyl)-triethoxysilane and 3-(azidopropyl)trimethoxysilane were prepared from the respective iodides (Gelest) and sodium azide in DMF and extracted into anhydrous hexanes.[18] The two azides behaved nominally identically in subsequent steps. No attempt was made to remove all DMF solvent as it assisted in grafting. Alkyl azides were grafted to solids by heating at 70−75 °C in sealed ~0.1 M toluene solutions, corresponding to ~2 mmol azide per g of powder, overnight, followed by washing with >20 volumetric equivalents each in warm toluene, acetonitrile, water, additional acetonitrile, and benzene to yield N_3-silica, N_3-MSU, or N_3-quartz. Powders were dried at room temperature under dynamic vacuum overnight before further modification; plates were dried in flowing N_2. Alkyl azides were not successfully grafted to Si_3N_4 nanoparticles under these conditions.

Oligomers were coupled to the azide-covered surface using a modified Cu-catalyzed Huisgen dipolar coupling "click" procedure.[19] A ~50 mM solution of the oligomer in $CHCl_3$ was added to 1.1 equiv. of Cu in a 2:1 suspension of $Cu(SO_4)_2$ (0.15 M) and sodium ascorbate (0.075 M) in DMF to form a yellow solution, presumably generating the Cu-acetylide. Plates were immersed and azide-functionalized powders were added to yield suspensions with ~0.1 mmol 12mer or 0.5 mmol dimer per g, sealed in a vial and shaken overnight at room temperature. Shaking was preferred to stir-bar mixing as the latter ground the

(11) Lahiri, S.; Thompson, J. L.; Moore, J. S. *J. Am. Chem. Soc.* **2000**, *122*, 11315–11319.
(12) Brunsveld, L.; Meijer, E. W.; Prince, R. B.; Moore, J. S. *J. Am. Chem. Soc.* **2001**, *123*, 7978–7984.
(13) Tour, J. M. *Acc. Chem. Res.* **2000**, *33*, 791–804. Donhauser, Z. J.; Mantooth, B. A.; Kelly, K. F.; Bumm, L. A.; Monnell, J. D.; Stapleton, J. J.; Price, D. W.; Rawlett, A. M.; Allara, D. L.; Tour, J. M.; Weiss, P. S. *Science* **2001**, *292*, 2303–2307. Stapleton, J. J.; Harder, P.; Daniel, T. A.; Reinard, M. D.; Yao, Y. X.; Price, D. W.; Tour, J. M.; Allara, D. L. *Langmuir* **2003**, *19*, 8245–8255. Devadoss, C.; Bharathi, P.; Moore, J. S. *J. Am. Chem. Soc.* **1996**, *118*, 9635–9644.
(14) Lummerstorfer, T.; Hoffmann, H. *J. Phys. Chem. B* **2004**, *108*, 3963–3966. Ciampi, S.; Bocking, T.; Kilian, K. A.; James, M.; Harper, J. B.; Gooding, J. J. *Langmuir* **2007**, *23*, 9320–9329. Ostaci, R. V.; Damiron, D.; Capponi, S.; Vignaud, G.; Leger, L.; Grohens, Y.; Drockenmuller, E. *Langmuir* **2008**, *24*, 2732–2739. Guo, Z. M.; Lei, A. W.; Liang, X. M.; Xu, Q. *Chem. Commun.* **2006**, 4512–4514. Prakash, S.; Long, T. M.; Selby, J. C.; Moore, J. S.; Shannon, M. A. *Anal. Chem.* **2007**, *79*, 1661–1667. Collman, J. P.; Devaraj, N. K.; Chidsey, C. E. D. *Langmuir* **2004**, *20*, 1051–1053. Sandoval, J. E.; Pesek, J. *J. Anal. Chem.* **1991**, *63*, 2634–2641.
(15) Britcher, L.; Barnes, T. J.; Griesser, H. J.; Prestidge, C. A. *Langmuir* **2008**, *24*, 7625–7627.
(16) Elliott, E. L.; Ray, C. R.; Kraft, S.; Atkins, J. R.; Moore, J. S. *J. Org. Chem.* **2006**, *71*, 5282–5290.
(17) Armarego, W. L. F.; Perrin, D. D. *Purification of Laboratory Chemicals*, fourth ed.; Butterworth-Heinemann: Boston, 1996.
(18) Fu, Y. S.; Yu, S. J. *Angew. Chem., Int. Ed.* **2001**, *40*, 437–440.
(19) Rostovtsev, V. V.; Green, L. G.; Fokin, V. V.; Sharpless, K. B. *Angew. Chem., Int. Ed.* **2002**, *41*, 2596.

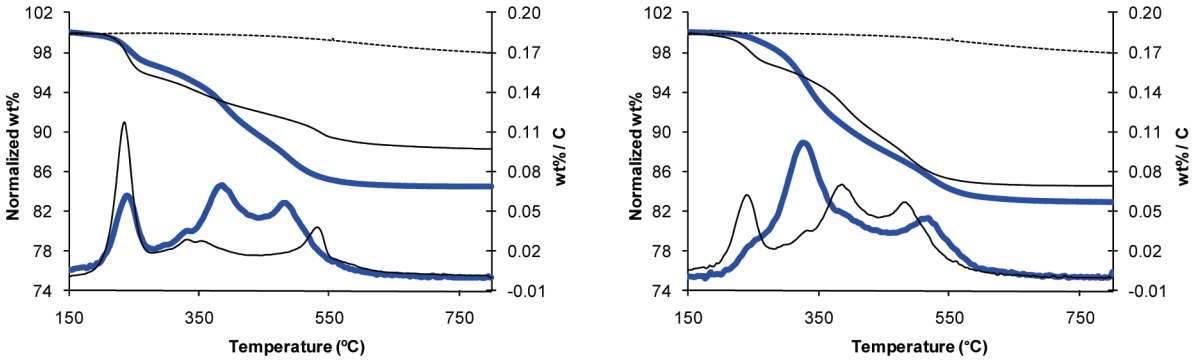

Figure 1. Thermogravimetric analysis and derivatives of materials synthesized by the coupling route. (left) N_3-silica and dimer-N_3-silica (bold); (right) dimer-N_3-silica and TMS-dimer-N_3-silica (bold). After normalizing to 150 °C, mass loss relative to silica (dashed line, both graphs) determines mass loading of each type of species.

particles to unmanageable suspensions. Solids were washed or sonicated briefly with $CHCl_3$ and with >20 volume equivalents of DMF, 0.1 M sodium diethyldithiocarbamate (>10 equiv per catalytic metal) in DMF,[20] DMF, and methanol to yield X-N_3-Y, where X is dimer or 12mer and Y is silica, MSU, or quartz. Final powders were dried at room temperature under dynamic vacuum overnight; plates were dried in flowing N_2. Following synthesis, all solids were generally dark mustard-yellow. Color, presumably from Cu species, was effectively removed from the solids and from subsequent washes using the sodium diethyldithiocarbamate solution to yield nearly white powders or clear plates. Some silica powders were subsequently treated with excess iodotrimethylsilane (TMSI, Gelest) as a 0.25 M solution acetonitrile at 70 °C and washed in polar solvents to reduce unreacted azides to primary amines and to cap residual silanols, producing TMS-X-N_3-silica, where X is dimer or 12mer.

Grafting by Hydrosilylation. Silica gel and Si_3N_4 nanoparticles were modified with SiH groups for subsequent hydrosilylation. Trimethoxysilane (Gelest) was grafted by first heating in 1:4:70 HCl:H_2O:dioxane at 70 °C under N_2 for 30 min, followed by dropwise addition of 0.5 M triethoxysilane in dioxane.[21] Each gram of powder was suspended in 20−40 mL of the reaction solution and refluxed overnight under N_2. The powders were washed with 1:4 H_2O:dioxane, dioxane, and ethyl ether, followed by drying for >4 h under dynamic vacuum at room temperature to generate H-silica and H−Si_3N_4. Methyldimethoxysilane (Gelest) was grafted by heating sealed vials at 70 °C for >24 h in 0.2 M toluene solutions containing >3 mmol silane per g of powder, followed by washing in dry THF and drying for >4 h under dynamic vacuum at room temperature to generate HC-silica.

Oligomers were coupled to SiH-modified surfaces using Rh-catalyzed hydrosilylation.[22] $RhI(PPh_3)_3$ was synthesized according to literature from triphenylphosphine, (Strem) $RhCl_3$ (Strem) and LiI.[23] Solid $RhI(PPh_3)_3$, the powder, and neat oligomer were added to a vial and toluene was added to make an oligomer concentration of 1 mM. Due to the small sample quantities synthesized, ~0.25 equiv. of Rh per terminal alkyene were employed, in vast excess compared to the 0.1 mol % required to observe successful hydrosilylation of model compounds in the presence of unfunctionalized silica gel. The vial was sealed under Ar and stirred for >4 h at 70 °C. The powders were subsequently washed with >20 volume equivalents of $CHCl_3$, 0.1 M diethaminodithiocarbamide (>10 equiv. per catalytic metal) in DMF, DMF, and $CHCl_3$, followed by drying for >4 h under dynamic vacuum at room temperature to yield X-HC-silica, X-H-silica, or X-H-Si_3N_4, where X is dimer or 12mer. Following synthesis, all solids were generally dark green. Color, presumably from Rh species, was effectively removed from the solids and from subsequent washes using the sodium diethyldithiocarbamate solution to yield faint yellow powders. Plates were not successfully grafted following this procedure.

Characterization. Thermogravimetric analyses (TGA) were carried out in a TGA/SDTA 851e in a flow of 99.995% synthetic air with a ramp rate of 10 °C/min to 800 °C. Photoluminescence spectra (Photon Technology International QM-1 with stirring or an ISS PC1 Photon Counting Spectrofluorimeter with stirring and temperature control), were acquired on suspensions of powders such that the averaged oligomer concentration was ~5 μM. Powders were diluted 10:1 with additional unfunctionalized silica gel to facilitate weighing. 2−4 scans were averaged to reduce signal noise arising from the random transiting of particles into the path of the excitation beam and all materials were tested in duplicate. Transmission UV−visible spectroscopy was performed using a Shimazdu 160A at ambient conditions on free-standing quartz chips. Two-nanometer slits were employed for improved signal-to-noise. Diffuse reflectance infrared Fourier transform spectra (DRIFTS) of the modified powders were averaged over 100 scans with a resolution of 8 cm^{-1} using the SMART diffuse reflectance accessory for the Nicolet 6700 and a background of the unmodified powders. Nitrogen physisorption was carried out using a Micromeritics ASAP 2010 with a preliminary 4 h evacuation at 150 °C. Transmission electron microscopy was carried out at the Northwestern EPIC facility of the NUANCE Center using a Hitachi H-8100 TEM.

Results and Discussion

Physical Characterization. Thermogravimetric analysis in dry air determines molar loadings on the various powder materials via combustion of the surface species. Representative TGA and derivative curves are given in Figures 1 and 2. Additional TGA curves are available in the Supporting Information. Mass losses are normalized to 150 °C, which is before ligand decomposition but after loss of variable amounts of residual solvent and water. The azide decomposes sharply near 230 °C, the triazole-tethered oligo(mPE) decomposes from 300 to 400 °C and

(20) Nielsen, K. T.; Spanggaard, H.; Krebs, F. C. *Macromolecules* **2005**, *38*, 1180–1189.
(21) Chu, C. H.; Jonsson, E.; Auvinen, M.; Pesek, J. J.; Sandoval, J. E. *Anal. Chem.* **1993**, *65*, 808–816.
(22) Mori, A.; Takahisa, E.; Yamamura, Y.; Kato, T.; Mudalige, A. P.; Kajiro, H.; Hirabayashi, K.; Nishihara, Y.; Hiyama, T. *Organometallics* **2004**, *23*, 1755–1765.
(23) Osborn, J. A.; Jardine, F. H.; Young, J. F.; Wilkinson, G. *J. Chem. Soc. A* **1966**, 1711–1732.

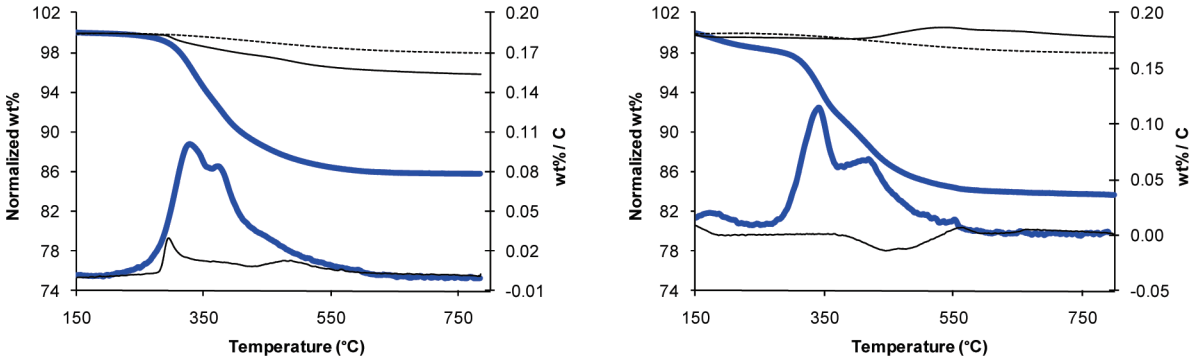

Figure 2. Thermogravimetric analysis and derivatives of materials synthesized by the hydrosilylation route. (left) HC-silica and 12mer-HC-silica (bold). (right) H-silica and 12mer-H-silica (bold). After normalizing to 150 °C, mass loss relative to silica (dashed line, both graphs) determines mass loading of each type of species.

Table 1. Oligomer Loadings and Surface Densities via Coupling and Hydrosilylation Methods

	azides		dimers			12mers		
support	loading (mmol/g)	density (per nm^2)	loading (mmol/g)	density (per nm^2)	% reaction (per anchor)	loading (mmol/g)	density (per nm^2)	% reaction (per anchor)
N_3-silica	1.2	1.6	0.34	0.45	28	0.003	0.004	< 1
N_3-MSU	1.7	1.6	0.23	0.19	12	0.009	0.008	< 1
N_3-quartz		n/d					0.22[a]	n/d
	SiH groups		dimers			12mers		
support	loading (mmol/g)	density (per nm^2)	loading (mmol/g)	density (per nm^2)	% reaction (per anchor)	loading (mmol/g)	density (per nm^2)	% reaction (per anchor)
HC-silica[b]	1.4	1.7	0.08	0.10	6	0.028	0.039	2
H-silica[c]	1.4	1.6	0.32	0.43	27	0.041	0.059	4
H−Si_3N_4[c]	n/d[d]	n/d	0.05	0.37	n/d	0.011	0.085	n/d

[a] Per side. [b] Via $SiCH_3H(OEt)_2$. [c] Via $SiH(OEt)_3$. [d] Mass changes insufficient to determine loading.

the silane decomposes from 400 to 500 °C. The azide peak area decreases with increasing oligomer grafting and is absent after treatment with the TMSI reducing agent. Trimethoxysilane shows a unique mass gain under oxidizing conditions at ~450 °C due to conversion of SiH to SiOH. Otherwise, TGA of SiH powders are similar to those of N_3 powders.

Table 1 details the stepwise assembly of species on these powders. Alkoxy silanes are grafted at ~1.6 groups per nm^2 regardless of support or functional group, which is a typical silane surface density.[24] Grafting efficiency of the dimer is maximized at ~28% with respect to either azides or silanes on silica, which is equivalent to a surface density of ~0.45 groups per nm^2 or an average separation of ~1.5 nm. Surface densities are referenced to the surface area of the original support before modification. The high surface density and its insensitivity to grafting chemistry suggest that the physical footprint of the grafted group, rather than surface accessibility or reactivity, limits deposition.

12mer grafting on powders occurs with up to 4% efficiency, or a surface density of up to 0.09 oligomers per nm^2, which is comparably crowded on a repeat unit basis to the dimer-modified surfaces. This grafting must occur on internal pores of the powders, because grafting this number of oligomers only on external powder surfaces would require physically unreasonable densities of 60−200 oligomers per nm^2 on the 0.3 to 0.1 m^2 g^{-1} of available external surface area. Grafting on azide-functionalized powders gives low surface coverages, which may reflect volume limitations of the larger tether or accumulation of oligomers or catalysts near pore mouths. Grafting densities are even lower when using typical lower concentrations of Cu catalyst. Decreased grafting has been observed previously with mesoporous silicon materials, and was ascribed to adsorption of Cu at the pore mouth by the high surface density of resulting trizoles.[15] Here, the product triazoles and the native silanols on the sparsely covered surfaces may both be serving to complex Cu, thus making it unavailable to catalyze the coupling reaction.

Nitrogen physisorption on 12mer-H-silica (Figure 3) shows a decrease in the total pore volume relative to H-silica of 0.13 cm^3/g. Using the loadings from Table 1, this gives an occluded volume of 5.2 nm^3 per molecule, or a density of 1.1 g cm^{-3} for grafted species contained within the pore space. Previous estimates of the density of oligomers in thin films have been between 1.04 and 1.2 g cm^{-3},[25,26] in line with that observed here. The similar calculated density indicates relatively uniform coverage of the pore surface, rather than blocking of pore mouths that would artificially

(24) Margelefsky, E. L.; Zeidan, R. K.; Davis, M. E. *Chem. Soc. Rev.* **2008**, *37*, 1118–1126.

(25) Kubel, C.; Mio, M. J.; Moore, J. S.; Martin, D. C. *J. Am. Chem. Soc.* **2002**, *124*, 8605–8610.

(26) Prest, P. J.; Prince, R. B.; Moore, J. S. *J. Am. Chem. Soc.* **1999**, *121*, 5933–5939.

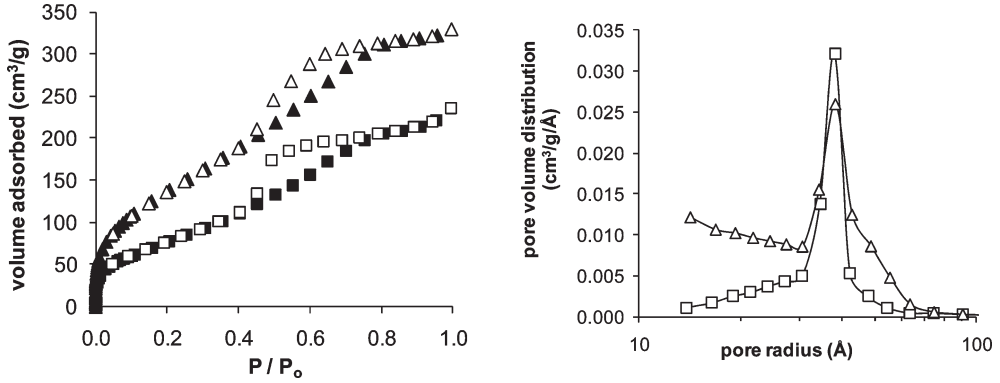

Figure 3. Adsorption (filled symbols) and desorption (open symbols) volumetric N_2 uptake (left) and BJH desorption pore size distributions (right) on 12mer-H-silica (■) and H-silica (▲). The difference in volumetric uptake indicates a density of 1.1 g cm^{-3} for the grafted 12mer. The pore size distribution of the silica support is narrowed by 12mer grafting, suggesting extended oligomers that penetrate micropores without blocking the mesopores.

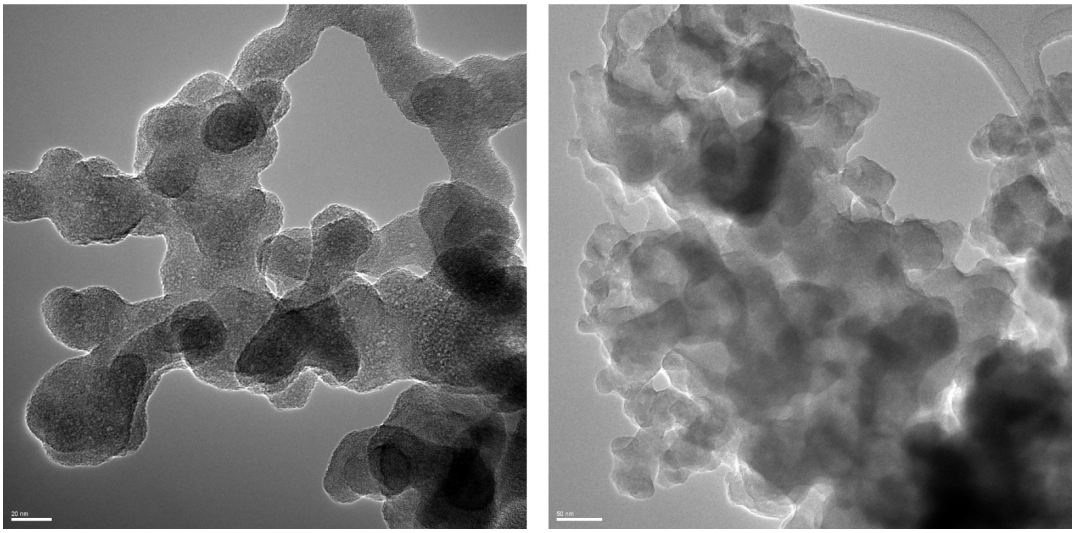

Figure 4. Transmission electron micrographs of H-Si_3N_4 (left, 20 nm bar) and 12mer-H-Si_3N_4 (right, 50 nm bar) showing change from smooth chains to rough aggregates with grafting.

deflate apparent densities. The grafted layer narrows the pore size distribution of the supporting silica gel (Figure 3), suggesting an extended conformation that penetrates micropores and smaller mesopores. Grafting 12mers on Si_3N_4 nanoparticles to create 12mer-H-Si_3N_4 decreases surface area from 110 to 90 m^2/g, consistent with coverage of the surface by the oligomers, but pore volumes and pore size distributions are not substantially altered (see Figure S2 in the Supporting Information), as expected for the macropores that arise only from interparticle voids in these aggregates of nanoparticles. Transmission electron micrographs (Figure 4) show that 12mer-H-Si_3N_4 exists as roughened aggregates, whereas the parent H-Si_3N_4 exists as smooth aggregates. The change in the morphology of the aggregates is consistent with a change in the surface chemistry after grafting.

Spectroscopy. Figure 5 shows the transmission UV−visible spectrum of the single monolayer of 12mer-N_3-quartz taken in air. The spectrum is comparable to published solution or thin film spectra.[26] This evidence of successful grafting of a monolayer onto the flat plates demonstrates, by extension, that grafting onto high surface area materials is indeed covalent, rather than simple physisorption into the pores. The

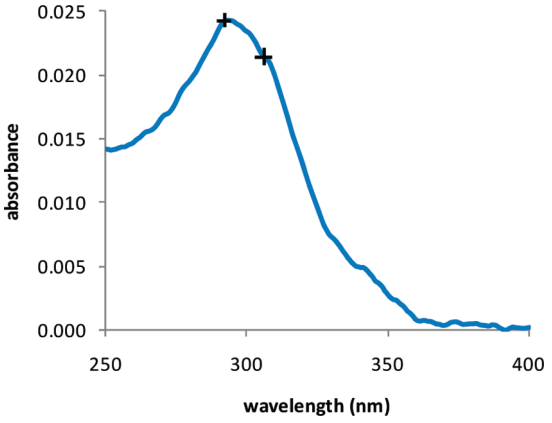

Figure 5. Transmission UV−visible spectrum of 12mer-N_3-quartz. Relative absorbances at 289 nm and 305 nm (marked) indicate an extended chain configuration. Absorbance intensity is consistent with a grafting density of 0.22 groups nm^{-2}.

intensity ratio of 305 to 289 nm has been previously used as an indicator of local environment by reporting the configurational change that accompanies solvophobic folding.[10] In air, the 12mer displays a high ratio of 0.88 characteristic of extended chains in $CHCl_3$ solution. Using a molar absorptivity

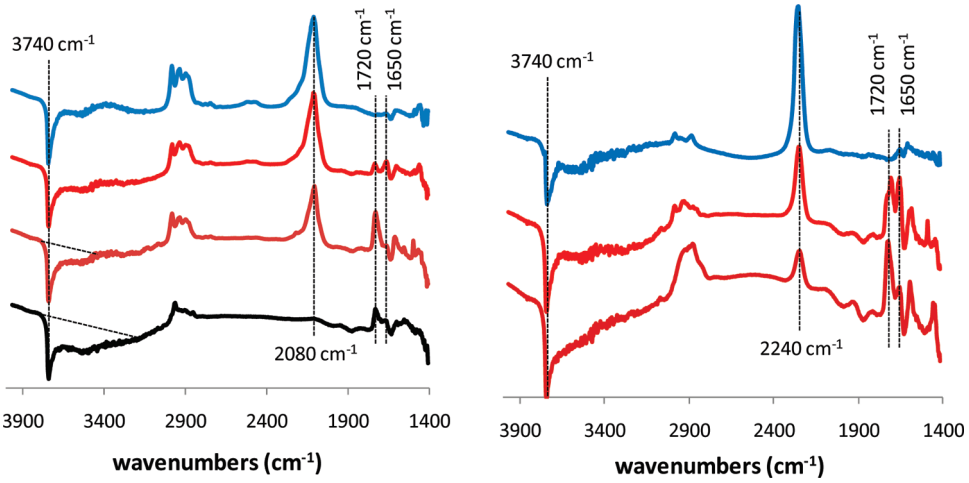

Figure 6. DRIFT spectra of materials synthesized by coupling (left) from top to bottom, N_3-silica, 12mer-N_3-silica, dimer-N_3-silica, and TMS-dimer-N_3-silica. DRIFT spectra of materials synthesized by hydrosilylation (right) from top to bottom, H-silica, 12mer-H-silica, and dimer-H-silica.

Scheme 2. Cartoon Depictions of 12mer Densities on Oxide Surfaces of Different Concavities

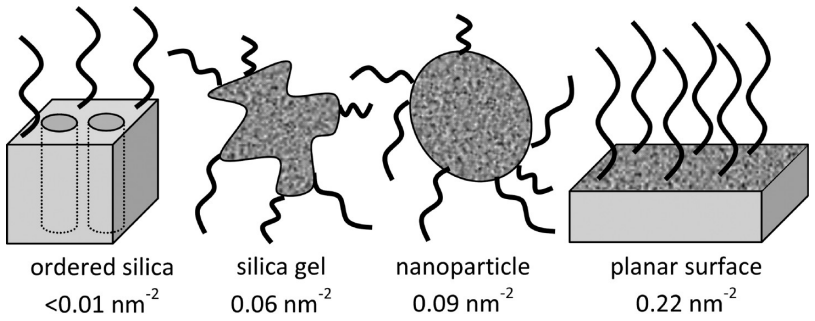

of $\sim 3 \times 10^5$ abs mmol^{-1}cm^2 previously determined for 12mer in solution,[27] the estimated surface density on the plate is 0.22 molecules per nm^2 per side, or an average molecular separation of 2.1 nm. This average spacing compares well with the lateral spacing enforced by the Tg groups in thin films of oligomers adopting extended chain conformations in lamellae.[26] The synthesis of these materials in a known unfolding solvent, $CHCl_3$, undoubtedly assists in the formation of densely packed extended chains.

Maximum achieved surface densities increase with increasingly planar surfaces. Inside the uniformly porous MSU silica, 12mer densities are <0.01 per nm^2, presumably because of restrictions at the pore mouth. 12mer densities reach 0.06 per nm^2 inside the disordered silica gel. On the nonporous, convex surfaces of Si_3N_4 nanoparticles, grafting densities are 0.09 per nm^2, and on macroscopically planar surfaces, densities reach 0.22 per nm^2, limited by the steric bulk of the molecule. This latter result does not indicate fully crystalline domains, which would pack at even higher densities due to close $\pi-\pi$ stacking perpendicular to the Tg groups, but rather something akin to a single monolayer smectic phase with liquidlike, extended chains aligned with the surface normal. (Scheme 2)

Figure 6 (left) shows the DRIFT spectra of N_3-silica, 12mer-N_3-silica, dimer-N_3-silica, and TMS-dimer-N_3-silica. All spectra are referenced to unfunctionalized silica. The negative peak at 3740 cm^{-1} represents the loss of isolated surface silanols upon grafting alkyl azides. Bands near 2900 cm^{-1} are assigned as C−H stretches from the alkyl azide and grafted oligomer. The strong vibration at 2080 cm^{-1} is consistent with azide N=N bonds. Grafting oligomers reduces this peak, and it is completely eliminated by reaction with TMSI that reduces azides to amines. Capping with TMSI also increases the negative signal from 3200 to 3600 cm^{-1}, indicating loss of H-bonded surface silanols and demonstrating accessibility of the silica surface after oligomer grafting. Figure 6 (right) shows the DRIFT spectra of H-silica, 12mer-H-silica, and dimer-H-silica relative to unfunctionalized silica. Silane grafting reduces the isolated silanol peak at 3740 cm^{-1}, and the SiH stretch appears at 2240 cm^{-1} and decreases in proportion to the number of oligomers successful grafted via hydrosilylation. In both sets of spectra, the vibration at 1720 cm^{-1} is consistent with ester C=O, and the vibration at 1650 cm^{-1} is consistent with either a triazole or alkene C=C bond arising from the surface connection. Variable amounts of undissociated adsorbed water, as a negative peak at 1620 cm^{-1}, make challenging the quantification of the C=C peaks, however, the large C=O peak for dimer-N_3-silica is consistent with the expected $>10\times$ number of ester groups in this material as compared to the 12mer-N_3-silica which grafted few repeat units.

(27) Stone, M. T.; Heemstra, J. M.; Moore, J. S. *Acc. Chem. Res.* **2006**, *39*, 11–20.

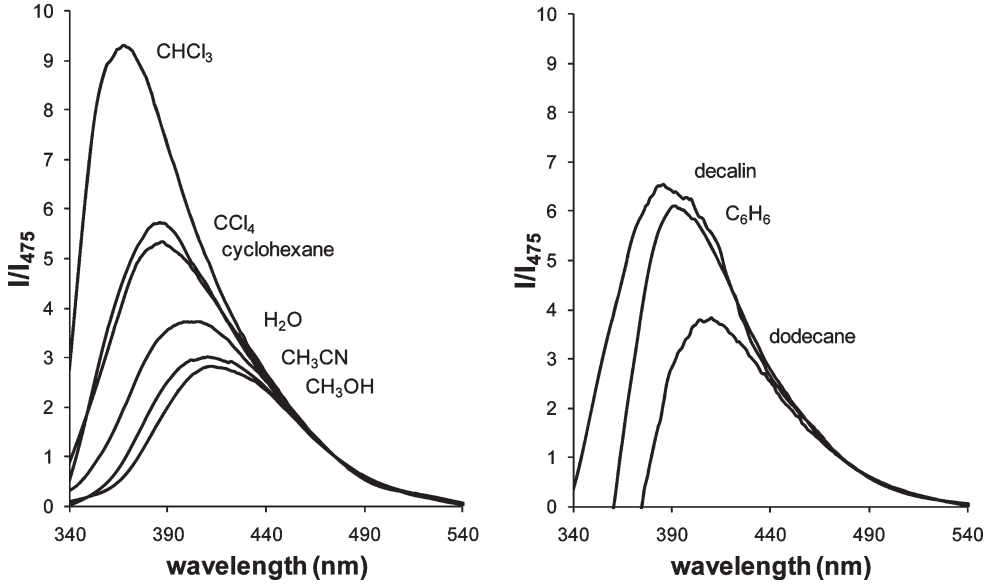

Figure 7. Room-temperature photoluminescence emission spectra (λ_{ex} = 289 nm) of 12mer-HC-silica in nine liquids normalized to the intensity at 475 nm. The spectra for dodecane, benzene, and decalin require a baseline correction because of background photoluminescence of those liquids.

Table 2. Photoluminescence Emission Relative Intensities and Wavelengths of Emission Maximum for a Liquid Panel, As Compared to Folding in Solution and a Common Solvent Scale

	liquid	$\lambda_{em,max}$	I_{max}/I_{475}	$\varepsilon_{305}/\varepsilon_{289}$[a]	E_T^{N}[b]
folding	CH_3OH	412	2.82	0.61	0.76
	CH_3CN	410	3.01	0.67	0.46
	H_2O	405	3.72		1.00
	dodecane	409	3.83		0.01
	cyclohexane	387	5.34		0.01
	CCl_4	386	5.73	0.78	0.05
	C_6H_6	391	6.10		0.11
	decalin	385	6.54		0.01
unfolding	$CHCl_3$	368	9.31	0.94	0.26

[a] From ref 29. [b] From ref 31.

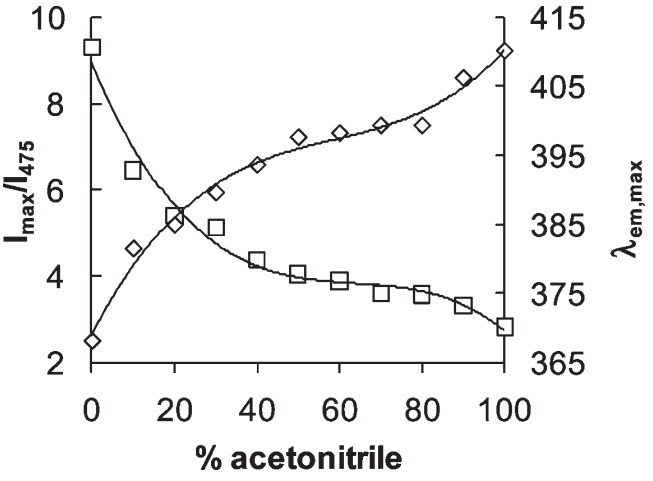

Figure 8. Smooth relationships in photoluminescence emission I_{max}/I_{475} and $\lambda_{em,max}$ (λ_{ex} = 289 nm) are observed for 12mer-HC-silica as a function of acetonitrile and are characteristic of an evolving population of two coexisting species. Lines are guides to the eye.

Association Behavior. Photoluminescence spectroscopy for particles in suspension was carried out to assess the association behavior of grafted oligomers. Soluble m-phenylene ethynylene oligomers are characterized by a relatively sharp emission at high energy (~350 nm) in unfolding solvents such as $CHCl_3$, and a broader, lower energy transition (~410 nm) in folding solvents such as acetonitrile.[11,27,28] Folding is a result of solvophobic interactions favoring intrachain $\pi-\pi$ stacking in poor solvents. Characteristic emission spectra (λ_{ex} = 289 nm) of 12mer-HC-silica in a panel of liquids is given in Figure 7. Spectra are normalized to the emission intensity at 475 nm, far from any emission maxima, to account for changes in powder settling due to different liquid viscosities that in turn changes apparent molar emissivity. Because the 12mers are covalently dispersed across the surface of the particle, and the particle is dispersed in any arbitrary fluid, association is studied for liquids in which the 12mer would not be normally soluble, such as water or dodecane.

Figure 7 shows that, as in solution, the wavelength and intensity of the maximum emission shifts smoothly between 355 and 420 nm for less or more folding liquids, respectively. Table 2 shows that the maximum relative emission intensity (I_{max}/I_{475}) and its wavelength ($\lambda_{em,max}$) trends with tabulated absorption spectra intensity ratios $\varepsilon_{305}/\varepsilon_{289}$ of soluble 12mer in CH_3OH, CH_3CN, CCl_4, and $CHCl_3$ that have been previously used to indicate folding or unfolding.[29] Grafting the oligomers to the solid surfaces

(28) Prince, R. B.; Saven, J. G.; Wolynes, P. G.; Moore, J. S. *J. Am. Chem. Soc.* **1999**, *121*, 3114–3121.

(29) Hill, D. J.; Moore, J. S. *Proc. Natl. Acad. Sci. U.S.A.* **2002**, *99*, 5053–5057.

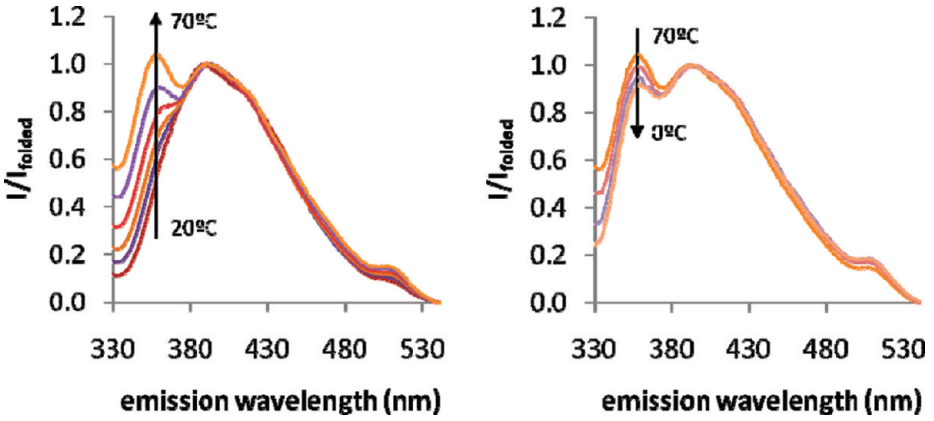

Figure 9. Photoluminescence emission spectra (λ_{ex} = 289 nm) of 12mer-HC-silica in CH_3CN upon heating (left) and cooling (right) normalized to the intensity at 390−405 nm showing evolution of the extended conformer with photoluminescence near 358 nm.

extends the investigation of folding to additional liquids in which the 12mer is insoluble or in which absorption spectra cannot be taken (benzene, water, decalin, dodecane, and cyclohexane), without requiring sidegroup elaboration.[30] The empirical solvent polarity measure[31] E_T^N has been previously used to correlate solvophobic folding behavior.[29] Here, however, photoluminescence in water (E_T^N = 1.0) and dodecane (E_T^N = 0.01) both indicate tightly associating structures, likely intermolecular, consistent with backbone and sidegroup insolubility in these solvents. In contrast, decalin and cyclohexane, both E_T^N = 0.01, give moderately unfolded oligomers, likely due to structural compatibility between solvent and oligomer. Even at its high surface densities, dimer-H-silica gives spectra characteristic of unfolded, solvated species in both $CHCl_3$ and CH_3CN (I_{max}/I_{475} = 5.2 and 7.9, respectively and λ_{max} = 370 and 365 nm, respectively), verifying that emissivity quenching does not arise purely from interchain association for these grafted species.

Using the metrics described above, solvent mixtures of $CHCl_3$ and CH_3CN show a monotonic relationship between I_{max}/I_{475} and solvent composition (Figure 8), but the relationship is not the characteristic sigmoidal shape observed free in solution and indicative of highly cooperative transformations.[11,28] Several differences between the solid-supported and solution species can be responsible for this difference, including the interplay of inter- and intramolecular association at the high local concentrations of the surface-grafted species and an adsorbed solvent phase composition that may differ from the bulk. The intrinsic heterogeneity of the surface of a porous solid particle is likely primarily responsible for the shape of this curve, which is consistent with the gradual evolution of mutually coexisting forms over a wide range of conditions. Following this pattern, at greater than 50% $CHCl_3$, a pronounced shoulder appears near 355 nm, similar to that seen in Figure 9 for CH_3CN at high temperatures, which grows in intensity alongside the most intense

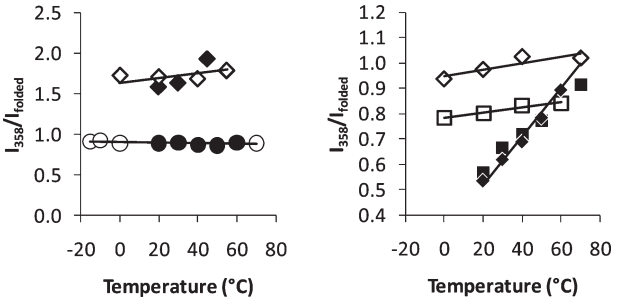

Figure 10. Relative photoluminescence emission I_{358}/I_{folded} (λ_{ex} = 289 nm, folded intensity is taken at the maximum between 390 and 405 nm), serving for a proxy of amount unfolded, during heating from room temperature (closed symbols) and subsequent cooling (open symbols). 12mer-HC-silica in $CHCl_3$ (◊, left) or CH_3CN (◊, right). 12mer-N_3-silica in CH_3CN (○, left) 12mer-HC-silica in 2 mM (+)-α-pinene/CH_3CN (□, right). Note the different intensity scales.

emission, which shifts smoothly from 410 to 370 nm with increasing $CHCl_3$ content.

Temperature-dependent folding behavior was also analyzed by photoluminescence in CH_3CN and $CHCl_3$ as a function of grafting type and external guests. These spectra also show the coexistence of two states under certain conditions. For 12mer-HC-silica in CH_3CN, a peak is observed at 390−405 nm with a shoulder transforming into a peak near 358 nm at increasing temperatures (Figure 9). Materials are suspended in $CHCl_3$ for at least 1 h before first acquisition and are subsequently stable indefinitely at room temperature. However, upon slow cooling from 70 °C, spectra are not reversible, suggesting that metastable configurations are able to be locked in during synthesis, and that significant activation barriers exist with respect to formation of the more stable surface structures. In these experiments, cooling takes place over several hours, and spectra are again stable at completion.

The ratio of the intensities at 358 nm and the maximum between 390 and 405 nm that is characteristic of folded species (I_{358}/I_{folded}) is used for these experiments as a proxy for the extent of folding instead of overall intensity, which is strongly temperature dependent due to different amounts of solid that is suspended as the liquid viscosity changes with temperature. This value is highest for

(30) Stone, M. T.; Moore, J. S. *Org. Lett.* **2004**, *6*, 469–472.
(31) Reichardt, C. *Solvents and Solvent Effects in Organic Chemistry*; VCH: New York, 1990.

unfolded chains. Figure 10 shows that 12mer-HC-silica is more unfolded at all temperatures probed in $CHCl_3$ than in CH_3CN. Spectral changes with temperature are weak and fully reversible in $CHCl_3$, as observed in free solution.[12] The emission ratios of highly loaded dimer-HC-silica are weakly dependent on temperature in both solvents demonstrating again that temperature-dependent behavior is not purely driven by intermolecular association. For 12mer-N_3-silica, with its low average density of 12mers and longer tether to the surface, temperature dependent changes are weak and fully reversible. However, as seen in Figure 9, highly loaded and more constrained 12mer-HC-silica in CH_3CN shows irreversible unfolding behavior upon heating from 20 to 70 °C; no unfolding was observed over several hours at 20 °C and the spectra did not revert after slow cooling. Thus, the room temperature configuration on the surface is influenced by the thermodynamic solvation behavior, but pronounced kinetic barriers may exist, and intermolecular association at these high surface densities may also inhibit expected intramolecular association behavior.[12] With additional thermal energy, an appreciable fraction of the 12mers constrained in porous silica gel are able to achieve the extended chain, unfolded configurations seen when supported on planar surfaces (vide supra).

In the folded state, oligo(mPE) is a known host for small molecule guests such as pinene,[7,30] and small molecules have been observed to have a templating effect that enhances folding.[8] After a heating and cooling cycle (Figure 10, right), the photoluminescence spectra of 12mer-HC-silica in 2 mM (+)-α-pinene in CH_3CN show reduced I_{358}/I_{folded} ratios, indicative of more tightly folded structures than for CH_3CN alone. As with the other thermal effects, no change in folding was observed after holding at 20 °C for several hours in the presence of guest (+)-α-pinene, nor did spectra revert after slow cooling. This result provides initial evidence that such grafted species may lead to the development of adsorbent surfaces that can be made responsive to adsorbates, much like natural protein receptors. Grafted foldamers may be ideal surfaces for the uptake of π-rich molecules such as polyaromatic hydrocarbons and fullerenes.

Conclusions

Oligomeric (mPE) have been grafted to high surface area and porous oxides by two techniques. Hydrosilylation based grafting gives up to a 15 wt % loading of this conjugated material, which is covalently grafted intact and retains the solvophobic association behavior characteristic of these foldamers. The solvophobic association is kinetically trapped in CH_3CN and strongly surface density dependent, since at high surface densities, the effective local concentration is ~50 mM, substantially higher than is required for aggregation. Addition of complementary molecules such as pinene can enhance folding, indicative of host−guest behavior on the surface. Attachment to the surface also allows very poor solvents to be tested for their folding behavior. Cyclohexane and decalin are somewhat unfolding solvents, in spite of their very low polarity and the poor solubility of the oligomers. These and related hybrid materials may have applications for host−guest-based selective adsorption or for energy transfer between the oligo(PE) and semiconductor oxide surfaces.

Acknowledgment. J.M.N. thanks Northwestern University and NSF CBET 0933667, and C.C. acknowledges support by the Institute for Atom-Efficient Chemical Transformation, an Energy Frontier Research Center funded by DOE BES. The authors thank Dr. Ron Smaldone for invaluable assistance with solid-phase synthesized 12mer. TEM was performed at the EPIC facility of NUANCE Center at Northwestern University. NUANCE Center is supported by NSF-NSEC, NSF-MRSEC, Keck Foundation, the State of Illinois, and Northwestern University.

Supporting Information Available: Additional thermogravimetric and N_2 physisorption analyses, and additional TEM images (PDF). This material is available free of charge via the Internet at http://pubs.acs.org.